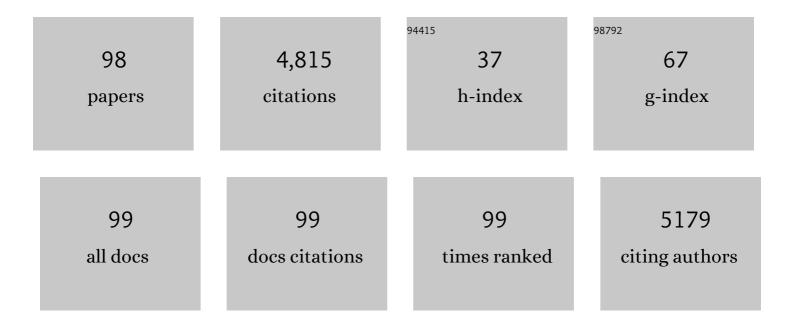
## Bhanu Bhusan Khatua

List of Publications by Year in descending order

Source: https://exaly.com/author-pdf/3006584/publications.pdf

Version: 2024-02-01



#	Article	IF	CITATIONS
1	Advanced self-charging power packs: The assimilation of energy harvesting and storage systems. , 2022, , 441-477.		1
2	Advanced functional materials and devices for energy conversion and storage applications. , 2022, , 43-96.		2
3	A microstructure-driven magnetic composite for excellent microwave absorption in extended Ku-band. Journal of Materials Chemistry C, 2022, 10, 3863-3875.	5.5	9
4	Comparative supercapacitive analysis of 2-methylimidazole derived cobalt nickel oxides (CoNiO2 and) Tj ETQq0 C Storage, 2022, 52, 104993.	0 rgBT /C 8.1	Verlock 10 T 4
5	Fabrication of a flexible quasi-solid-state asymmetric supercapacitor device based on a spherical honeycomb like ZnMn2O4@Ni(OH)2 hybrid core-shell electrode material with superior electrochemical performances. Results in Chemistry, 2022, 4, 100404.	2.0	5
6	An approach to designing smart future electronics using nature-driven biopiezoelectric/triboelectric nanogenerators. , 2021, , 251-282.		2
7	Autonomous self-repair in piezoelectric molecular crystals. Science, 2021, 373, 321-327.	12.6	72
8	Photovoltaic and triboelectrification empowered light-weight flexible self-charging asymmetric supercapacitor cell for self-powered multifunctional electronics. Renewable and Sustainable Energy Reviews, 2021, 151, 111595.	16.4	20
9	High performance alkaline battery-supercapacitor hybrid device based on diffusion driven double shelled CoSn(OH)6 nanocube@â^•Ni(OH)2 core-shell nanoflower. Journal of Energy Storage, 2021, 43, 103206.	8.1	5
10	A Quasi-Solid-State Asymmetric Supercapacitor Device Based on Honeycomb-like Nickel–Copper–Carbonate–Hydroxide as a Positive and Iron Oxide as a Negative Electrode with Superior Electrochemical Performances. ACS Applied Electronic Materials, 2020, 2, 177-185.	4.3	34
11	A polypyrrole-adorned, self-supported, pseudocapacitive zinc vanadium oxide nanoflower and nitrogen-doped reduced graphene oxide-based asymmetric supercapacitor device for power density applications. New Journal of Chemistry, 2020, 44, 1063-1075.	2.8	35
12	Nanostructured cigarette wrapper encapsulated <scp>PDMSâ€RGO</scp> sandwiched composite for high performance <scp>EMI</scp> shielding applications. Polymer Engineering and Science, 2020, 60, 3056-3071.	3.1	15
13	Approach for Enhancement in Output Performance of Randomly Oriented ZnSnO <sub>3</sub> Nanorod-Based Piezoelectric Nanogenerator via p–n Heterojunction and Surface Passivation Layer. ACS Applied Electronic Materials, 2020, 2, 2565-2578.	4.3	22
14	Recent Advances in Selfâ€Powered Triboâ€∤Piezoelectric Energy Harvesters: Allâ€Inâ€One Package for Future Smart Technologies. Advanced Functional Materials, 2020, 30, 2004446.	14.9	133
15	<i>In situ</i> -grown organo-lead bromide perovskite-induced electroactive γ-phase in aerogel PVDF films: an efficient photoactive material for piezoelectric energy harvesting and photodetector applications. Nanoscale, 2020, 12, 7214-7230.	5.6	44
16	A strategy to develop highly efficient TENGs through the dielectric constant, internal resistance optimization, and surface modification. Journal of Materials Chemistry A, 2019, 7, 3979-3991.	10.3	70
17	Fabrication of an Advanced Asymmetric Supercapacitor Based on Three-Dimensional Copper–Nickel–Cerium–Cobalt Quaternary Oxide and GNP for Energy Storage Application. ACS Applied Electronic Materials, 2019, 1, 189-197.	4.3	66
18	Highly Rate Capable Nanoflower-like NiSe and WO <sub>3</sub> @PPy Composite Electrode Materials toward High Energy Density Flexible All-Solid-State Asymmetric Supercapacitor. ACS Applied Electronic Materials, 2019, 1, 977-990.	4.3	86

#	Article	IF	CITATIONS
19	PVC bead assisted selective dispersion of MWCNT for designing efficient electromagnetic interference shielding PVC/MWCNT nanocomposite with very low percolation threshold. Composites Part B: Engineering, 2019, 167, 377-386.	12.0	39
20	Nature Driven Bioâ€Piezoelectric/Triboelectric Nanogenerator as Nextâ€Generation Green Energy Harvester for Smart and Pollution Free Society. Advanced Energy Materials, 2019, 9, 1803027.	19.5	111
21	Designing high energy conversion efficient bio-inspired vitamin assisted single-structured based self-powered piezoelectric/wind/acoustic multi-energy harvester with remarkable power density. Nano Energy, 2019, 59, 169-183.	16.0	107
22	Morphological interference of two different cobalt oxides derived from a hydrothermal protocol and a single two-dimensional metal organic framework precursor to stabilize the β-phase of PVDF for flexible piezoelectric nanogenerators. Nanoscale, 2019, 11, 22989-22999.	5.6	47
23	Triboelectric Nanogenerator Driven Self-Charging and Self-Healing Flexible Asymmetric Supercapacitor Power Cell for Direct Power Generation. ACS Applied Materials & Interfaces, 2019, 11, 5022-5036.	8.0	63
24	Graphene, Its Analogues, and Modern Science. Springer Proceedings in Physics, 2019, , 215-236.	0.2	0
25	Temperature dependent substrate-free facile synthesis for hierarchical sunflower-like nickel–copper carbonate hydroxide with superior electrochemical performance for solid state asymmetric supercapacitor. Chemical Engineering Journal, 2018, 343, 44-53.	12.7	38
26	A strategy to develop an efficient piezoelectric nanogenerator through ZTO assisted γ-phase nucleation of PVDF in ZTO/PVDF nanocomposite for harvesting bio-mechanical energy and energy storage application. Materials Chemistry and Physics, 2018, 213, 525-537.	4.0	71
27	An approach to widen the electromagnetic shielding efficiency in PDMS/ferrous ferric oxide decorated RGO–SWCNH composite through pressure induced tunability. Chemical Engineering Journal, 2018, 335, 501-509.	12.7	67
28	Insight into Cigarette Wrapper and Electroactive Polymer Based Efficient TENG as Biomechanical Energy Harvester for Smart Electronic Applications. ACS Applied Energy Materials, 2018, 1, 4963-4975.	5.1	26
29	A new insight towards eggshell membrane as high energy conversion efficient bio-piezoelectric energy harvester. Materials Today Energy, 2018, 9, 114-125.	4.7	82
30	High performance advanced asymmetric supercapacitor based on ultrathin and mesoporous MnCo2O4.5-NiCo2O4 hybrid and iron oxide decorated reduced graphene oxide electrode materials. Electrochimica Acta, 2018, 283, 438-447.	5.2	47
31	Nature driven spider silk as high energy conversion efficient bio-piezoelectric nanogenerator. Nano Energy, 2018, 49, 655-666.	16.0	136
32	An Approach To Fabricate PDMS Encapsulated All-Solid-State Advanced Asymmetric Supercapacitor Device with Vertically Aligned Hierarchical Zn–Fe–Co Ternary Oxide Nanowire and Nitrogen Doped Graphene Nanosheet for High Power Device Applications. ACS Applied Materials & Interfaces, 2017, 9, 5947-5958.	8.0	81
33	A Mesoporous High-Performance Supercapacitor Electrode Based on Polypyrrole Wrapped Iron Oxide Decorated Nanostructured Cobalt Vanadium Oxide Hydrate with Enhanced Electrochemical Capacitance. Industrial & Engineering Chemistry Research, 2017, 56, 2444-2457.	3.7	42
34	Polyaniline/α-Ni(OH)2/iron oxide-doped reduced graphene oxide-based hybrid electrode material. Journal of Applied Electrochemistry, 2017, 47, 531-546.	2.9	12
35	Fabrication of an advanced asymmetric supercapacitor based on a microcubical PB@MnO <sub>2</sub> hybrid and PANI/GNP composite with excellent electrochemical behaviour. Journal of Materials Chemistry A, 2017, 5, 22242-22254.	10.3	75
36	Bio-waste onion skin as an innovative nature-driven piezoelectric material with high energy conversion efficiency. Nano Energy, 2017, 42, 282-293.	16.0	117

#	Article	IF	CITATIONS
37	Fast charging self-powered wearable and flexible asymmetric supercapacitor power cell with fish swim bladder as an efficient natural bio-piezoelectric separator. Nano Energy, 2017, 40, 633-645.	16.0	89
38	Salt leached viable porous Fe3O4 decorated polyaniline – SWCNH/PVDF composite spectacles as an admirable electromagnetic shielding efficiency in extended Ku-band region. Composites Part B: Engineering, 2017, 129, 210-220.	12.0	52
39	NaCl leached sustainable porous flexible Fe3O4 decorated RGO-polyaniline/PVDF composite for durable application against electromagnetic pollution. EXPRESS Polymer Letters, 2017, 11, 419-433.	2.1	23
40	Effect of Î <sup>3</sup> -PVDF on enhanced thermal conductivity and dielectric property of Fe-rGO incorporated PVDF based flexible nanocomposite film for efficient thermal management and energy storage applications. RSC Advances, 2016, 6, 37773-37783.	3.6	58
41	Optically transparent polycarbonate/clay nanocomposites with improved performance using phosphonium modified organoclay: Preparation and characterizations. Polymer Composites, 2016, 37, 199-212.	4.6	5
42	A Facile Approach To Develop a Highly Stretchable PVC/ZnSnO <sub>3</sub> Piezoelectric Nanogenerator with High Output Power Generation for Powering Portable Electronic Devices. Industrial & Engineering Chemistry Research, 2016, 55, 10671-10680.	3.7	75
43	An Approach to Design Highly Durable Piezoelectric Nanogenerator Based on Selfâ€Poled PVDF/AlOâ€rGO Flexible Nanocomposite with High Power Density and Energy Conversion Efficiency. Advanced Energy Materials, 2016, 6, 1601016.	19.5	324
44	Expanded graphite ( <scp>EG</scp> ) as a potential filler in the reduction of percolation threshold of multiwall carbon nanotubes ( <scp>MWCNT</scp> ) in the <scp>PMMA/HDPE/EG/MWCNT</scp> nanocomposites. Polymer Composites, 2016, 37, 2070-2082.	4.6	12
45	Graphene nanoplate and multiwall carbon nanotube–embedded polycarbonate hybrid composites: High electromagnetic interference shielding with low percolation threshold. Polymer Composites, 2016, 37, 2058-2069.	4.6	49
46	Green composites based on highâ€density polyethylene andSaccharum spontaneum: Effect of filler content on morphology, thermal, and mechanical properties. Polymer Composites, 2015, 36, 2157-2166.	4.6	13
47	High electromagnetic interference shielding with high electrical conductivity through selective dispersion of multiwall carbon nanotube in poly (ε aprolactone)/ <scp>MWCNT</scp> composites. Journal of Applied Polymer Science, 2015, 132, .	2.6	15
48	Reduction of percolation threshold of multiwall carbon nanotube (MWCNT) in polystyrene (PS)/lowâ€density polyethylene (LDPE)/MWCNT nanocomposites: An ecoâ€friendly approach. Polymer Composites, 2015, 36, 1574-1583.	4.6	13
49	Carbon nanohorn and graphene nanoplate based polystyrene nanocomposites for superior electromagnetic interference shielding applications. Journal of Applied Polymer Science, 2015, 132, .	2.6	29
50	Self-powered flexible Fe-doped RGO/PVDF nanocomposite: an excellent material for a piezoelectric energy harvester. Nanoscale, 2015, 7, 10655-10666.	5.6	303
51	Single wall carbon nanohorn (SWCNH)/graphene nanoplate/poly(methyl methacrylate) nanocomposites: a promising material for electromagnetic interference shielding applications. RSC Advances, 2015, 5, 70482-70493.	3.6	21
52	High Energy Density Ternary Composite Electrode Material Based on Polyaniline (PANI), Molybdenum trioxide (MoO3) and Graphene Nanoplatelets (GNP) Prepared by Sono-Chemical Method and Their Synergistic Contributions in Superior Supercapacitive Performance. Electrochimica Acta, 2015, 180, 1-15.	5.2	96
53	Facile preparation of highly exfoliated and optically transparent polycarbonate (PC)/clay mineral nanocomposites using phosphonium modified organoclay mineral. Applied Clay Science, 2014, 95, 182-190.	5.2	13
54	Low percolation threshold and high electrical conductivity in melt-blended polycarbonate/multiwall carbon nanotube nanocomposites in the presence of poly(ε-caprolactone). Polymer Engineering and Science, 2014, 54, 646-659.	3.1	23

Bhanu Bhusan Khatua

#	Article	IF	CITATIONS
55	An approach to reduce the percolation threshold of MWCNT in ABS/MWCNT nanocomposites through selective distribution of CNT in ABS matrix. RSC Advances, 2014, 4, 24584.	3.6	21
56	Highly exfoliated eco-friendly thermoplastic starch (TPS)/poly (lactic acid)(PLA)/clay nanocomposites using unmodified nanoclay. Carbohydrate Polymers, 2014, 110, 430-439.	10.2	147
57	Effect of nanoclay on the morphology and properties of acrylonitrile butadiene styrene toughened polyoxymethylene (POM)/clay nanocomposites. Polymer Composites, 2014, 35, 273-282.	4.6	26
58	A strategy to achieve high electromagnetic interference shielding and ultra low percolation in multiwall carbon nanotube–polycarbonate composites through selective localization of carbon nanotubes. RSC Advances, 2014, 4, 7979.	3.6	80
59	Reduction of percolation threshold through double percolation in meltâ€blended polycarbonate/acrylonitrile butadiene styrene/multiwall carbon nanotubes elastomer nanocomposites. Polymer Composites, 2013, 34, 570-579.	4.6	77
60	Phosphonium modified organoclay as potential nanofiller for the development of exfoliated and optically transparent polycarbonate/clay nanocomposites: Preparation and characterizations. European Polymer Journal, 2013, 49, 49-60.	5.4	31
61	Development of electrical conductivity in PP/HDPE/MWCNT nanocomposite by melt mixing at very low loading of MWCNT. Polymer Composites, 2013, 34, 787-798.	4.6	31
62	Electrochemical and electrical performances of cobalt chloride (CoCl2) doped polyaniline (PANI)/graphene nanoplate (GNP) composite. RSC Advances, 2013, 3, 12874.	3.6	33
63	Low percolation threshold in melt-blended PC/MWCNT nanocomposites in the presence of styrene acrylonitrile (SAN) copolymer: Preparation and characterizations. Synthetic Metals, 2013, 165, 40-50.	3.9	34
64	Polystyrene/MWCNT/Graphite Nanoplate Nanocomposites: Efficient Electromagnetic Interference Shielding Material through Graphite Nanoplate–MWCNT–Graphite Nanoplate Networking. ACS Applied Materials & Interfaces, 2013, 5, 4712-4724.	8.0	295
65	Low percolation threshold in polycarbonate/multiwalled carbon nanotubes nanocomposites through melt blending with poly(butylene terephthalate). Journal of Applied Polymer Science, 2013, 130, 543-553.	2.6	86
66	Ultralow Electrical Percolation Threshold in Poly(styrene- <i>co</i> -acrylonitrile)/Carbon Nanotube Nanocomposites. Industrial & Engineering Chemistry Research, 2013, 52, 2858-2868.	3.7	24
67	Positive temperature coefficient to resistively characteristics of polystyrene/nickel powder/multiwall carbon nanotubes composites. Polymer Composites, 2012, 33, 1977-1986.	4.6	3
68	Exfoliated and Optically Transparent Polycarbonate/Clay Nanocomposites Using Phosphonium Modified Organoclay: Preparation and Characterizations. Industrial & Engineering Chemistry Research, 2012, 51, 15096-15108.	3.7	11
69	A facile route to develop electrical conductivity with minimum possible multiâ€wall carbon nanotube (MWCNT) loading in poly(methyl methacrylate)/MWCNT nanocomposites. Polymer International, 2012, 61, 1683-1692.	3.1	21
70	Effect of nanoclay on positive temperature coefficient to resistivity characteristics of high density polyethylene/silverâ€coated glass bead composites. Polymer Composites, 2012, 33, 819-828.	4.6	7
71	Preparation of highly exfoliated and transparent polycarbonate/clay nanocomposites by melt blending of polycarbonate and poly(methyl methacrylate)/clay nanocomposites. Journal of Applied Polymer Science, 2012, 125, E601.	2.6	24
72	Morphology and properties of nylon 6 and high density polyethylene blends in presence of nanoclay and PEâ€gâ€MA. Journal of Applied Polymer Science, 2012, 123, 1801-1811.	2.6	29

#	Article	IF	CITATIONS
73	Electrical and mechanical properties of acrylonitrileâ€butadieneâ€styrene/multiwall carbon nanotube nanocomposites prepared by meltâ€blending. Journal of Applied Polymer Science, 2012, 124, 3165-3174.	2.6	26
74	PTCR characteristics of poly(styreneâ€ <i>co</i> â€acrylonitrile) copolymer/stainless steel powder composites. Journal of Applied Polymer Science, 2012, 124, 607-615.	2.6	8
75	Synthesis of highly exfoliated PS/Na+-MMT nanocomposites by suspension polymerization using Na+-MMT clay platelets as suspension stabilizer. Macromolecular Research, 2011, 19, 44-52.	2.4	15
76	Preparation by suspension polymerization and characterization of polystyrene (PS)-poly(methyl) Tj ETQq0 0 0 rg	;BT /Overlo 2.4	ock 10 Tf 50 6 34
77	PTCR characteristics of polycarbonate/nickelâ€coated graphiteâ€based conducting polymeric composites in presence of poly(caprolactone). Polymer Composites, 2011, 32, 747-755.	4.6	12
78	Highly reversible and repeatable PTCR characteristics of PMMA/Agâ€coated glass bead composites based on CTE mismatch phenomena. Polymer Engineering and Science, 2011, 51, 1780-1790.	3.1	19
79	Cocontinuous phase morphology of asymmetric compositions of polypropylene/highâ€density polyethylene blend by the addition of clay. Journal of Applied Polymer Science, 2011, 119, 3080-3092.	2.6	35
80	Morphology and properties of nylon6 and high density polyethylene blends in absence and presence of nanoclay. Journal of Applied Polymer Science, 2011, 121, 359-368.	2.6	23
81	Development of electrical conductivity with minimum possible percolation threshold in multi-wall carbon nanotube/polystyrene composites. Carbon, 2011, 49, 4571-4579.	10.3	82
82	Properties of Polycarbonate (PC)/Multi-Wall Carbon Nanotube (MWCNT) Nanocomposites Prepared by Melt Blending. Journal of Nanoscience and Nanotechnology, 2011, 11, 8613-8620.	0.9	7
83	Effect of Nanoclay and SEBS-g-MA on the Morphology and Properties of Immiscible Poly(methyl) Tj ETQq1 1 0.7	84314 rgB 0.9	T /gverlock 1
84	Thermal and Rheological Properties of Biodegradable Poly[(butylene succinate)-co-adipate] Nanocomposites. Journal of Nanoscience and Nanotechnology, 2010, 10, 4184-4195.	0.9	17
85	Preparation and Characterization of Poly(methyl methacrylate)/Multi-Walled Carbon Nanotube Composites. Journal of Nanoscience and Nanotechnology, 2009, 9, 4644-4655.	0.9	25
86	Multi-Walled Carbon Nanotubes/Polymer Composites in Absence and Presence of Acrylic Elastomer (ACM). Journal of Nanoscience and Nanotechnology, 2009, 9, 2981-2990.	0.9	7
87	Use of Pristine Clay Platelets as a Suspension Stabilizer for the Synthesis of Poly(methyl) Tj ETQq1 1 0.784314 r	gBT_ <i>l</i> Overl	ock 10 Tf 50
88	Macromol. Chem. Phys. 13-14/2009. Macromolecular Chemistry and Physics, 2009, 210, NA-NA.	2.2	0
89	Effect of clay platelet dispersion as affected by the manufacturing techniques on thermal and mechanical properties of PMMAâ€clay nanocomposites. Journal of Applied Polymer Science, 2009, 113, 3012-3018.	2.6	34
90	Synergistic Effect of Nanoclay and EPR-g-MA on the Properties of Nylon6/EPR Blends. Journal of Nanoscience and Nanotechnology, 2009, 9, 3099-3105.	0.9	1

BHANU BHUSAN KHATUA

#	Article	IF	CITATIONS
91	Mechanical, morphological and thermal properties of in situ ternary composites based on poly(ether) Tj ETQq1 1 Structural Materials: Properties, Microstructure and Processing, 2008, 490, 198-207.	0.784314 5.6	rgBT /Ove 19
92	Studies on nylon-6/EVOH/clay ternary composites. Polymer Composites, 2006, 27, 15-23.	4.6	6
93	Aging behavior of oxygen plasma-treated polypropylene with different crystallinities. Journal of Adhesion Science and Technology, 2004, 18, 1279-1291.	2.6	80
94	Investigation of surface molecular orientation of poly(dimethylsiloxane-co-diphenylsiloxane)-modified poly(amic acid) films using dynamic contact angle measurements, NEXAFS and XPS. Journal of Adhesion Science and Technology, 2004, 18, 1815-1831.	2.6	4
95	Interchain crosslinkable polymer blends of polyurethane and polyacrylic elastomer (sulfur cure). Journal of Applied Polymer Science, 2004, 93, 845-853.	2.6	0
96	Effect of Organoclay Platelets on Morphology of Nylon-6 and Poly(ethylene-ran-propylene) Rubber Blends. Macromolecules, 2004, 37, 2454-2459.	4.8	350
97	Thermally crosslinked polymer blends of polyurethane and chlorobutyl elastomers (sulfur cure). Polymer International, 2001, 50, 495-502.	3.1	2
98	Polyblend systems of polyurethane (AU) and ethylene acrylic elastomer (vamac) using the sulfur cure systems. Journal of Applied Polymer Science, 2001, 80, 2737-2745.	2.6	4